

A Cathepsin D-Cleaved 16 kDa Form of Prolactin Mediates Postpartum Cardiomyopathy

Denise Hilfiker-Kleiner,¹ Karol Kaminski,¹ Edith Podewski,¹ Tomasz Bonda,¹ Arnd Schaefer,¹ Karen Sliwa,³ Olaf Forster,³ Anja Quint,¹ Ulf Landmesser,¹ Carola Doerries,¹ Maren Luchtefeld,¹ Valeria Poli,⁴ Michael D. Schneider,⁵ Jean-Luc Balligand,⁶ Fanny Desjardins,⁶ Aftab Ansari,⁷ Ingrid Struman,⁸ Ngoc Q.N. Nguyen,⁸ Nils H. Zschemisch,¹ Gunnar Klein,¹ Gerd Heusch,⁹ Rainer Schulz,⁹ Andres Hilfiker,^{1,2} and Helmut Drexler¹

¹ Department of Cardiology and Angiology

² Department of Thoracic and Cardiovascular Surgery MHH, 30625 Hannover, Germany

³ Department of Cardiology, Chris-Hani-Baragwanath Hospital, University of the Witwatersrand, 2013 Soweto, South Africa

⁴ Department of Genetics, Biology, and Biochemistry, University of Turin, 10126 Turin, Italy

⁵ Department of Medicine, Baylor College of Medicine, Houston, TX 77030, USA

⁶ Department of Pharmacology and Therapeutics, University of Louvain Medical School, 1200 Brussels, Belgium

⁷ Department of Pathology and Laboratory Medicine, Emory University, Atlanta, GA 30322, USA

⁸ Centre of Biomedical Integrative Genoproteomics, Université de Liege, 4000 Sart Tilman, Belgium

⁹ Department of Pathophysiology, Universitaetsklinikum, Essen, 45122 Essen, Germany

SUMMARY

Postpartum cardiomyopathy (PPCM) is a disease of unknown etiology and exposes women to high risk of mortality after delivery. Here, we show that female mice with a cardiomyocyte-specific deletion of *stat3* develop PPCM. In these mice, cardiac cathepsin D (CD) expression and activity is enhanced and associated with the generation of a cleaved antiangiogenic and proapoptotic 16 kDa form of the nursing hormone prolactin. Treatment with bromocriptine, an inhibitor of prolactin secretion, prevents the development of PPCM, whereas forced myocardial generation of 16 kDa prolactin impairs the cardiac capillary network and function, thereby recapitulating the cardiac phenotype of PPCM. Myocardial STAT3 protein levels are reduced and serum levels of activated CD and 16 kDa prolactin are elevated in PPCM patients. Thus, a biologically active derivative of the pregnancy hormone prolactin mediates PPCM, implying that inhibition of prolactin release may represent a novel therapeutic strategy for PPCM.

INTRODUCTION

Postpartum cardiomyopathy (PPCM) is a disease of unknown etiology, characterized by an acute onset of heart failure in women in the late stage of pregnancy up to several months postpartum, resulting in high mortality despite optimal medical therapy (Elkayam et al., 2005; Reimold and Rutherford, 2001 ; Sliwa et al., 2002).

In PPCM patients, serum markers of inflammation and apoptosis are significantly elevated, which appears to predict impaired functional status and mortality, consistent with the idea that inflammation and apoptosis may contribute to the pathogenesis of PPCM (Sliwa et al., 2006; Sliwa et al., 2002). In line with these clinical observations, it has been shown that transgenic mice with cardiac-specific overexpression of the α subunit of Gq develop PPCM, which could be attenuated by pharmacological inhibition of apoptosis (Hayakawa et al., 2003).

We noted that female mice with a homozygous or heterozygous cardiomyocyte-specific knockout of STAT3 (*aMHC-cre*^{+/-}; *stat3*^{lox/lox}: CKO; *aMHC-cre*^{+/-}; *stat3*^{lox/+}: HET) develop PPCM in a dose-dependent manner (CKO > HET). Notably, STAT3 is involved in protection of the heart from oxidative stress by upregulation of antioxidative enzymes such as the reactive oxygen species (ROS) scavenging enzyme manganese superoxide dismutase (MnSOD) (Negoro et al., 2001). STAT3 also plays an important role in promoting myocardial angiogenesis both by paracrine and autocrine mechanisms in cardiomyocytes and nonmyocytes (Bartoli et al., 2003; Hilfiker-Kleiner et al., 2004a; Osugi et al., 2002), and it can mediate cardiomyocyte hypertrophy (Hilfiker-Kleiner et al., 2004a; Kunisada et al., 2000). In the present study, we used the above genetic mouse model to investigate potential underlying mechanisms, which may initiate and/or drive PPCM. We found a detrimental link between enhanced oxidative stress and cleavage of the pregnancy hormone prolactin (PRL) into an antiangiogenic 16 kDa form (Corba-cho et al., 2002; Tabruyn et al., 2003) as a major cause of PPCM. Furthermore, we explored similarities between PPCM in mice and humans and initiated a novel therapeutic strategy with the PRL inhibitor bromocriptine in woman with a high risk of developing PPCM.

Table 1: HW:BW, Cardiac Dimensions, and Function in NT and CKO Female Mice Postpartum with or without Treatment with BR

	NP		PP		PP/BR	
	NT	CKO	NT	CKO	NT	CKO
HW:BW (mg:g)	3.8 ± 0.5	3.7 ± 0.3	4.6 ± 0.5*	5.5 ± 1.2*#	4.1 ± 0.5	4.5 ± 0.7**
LVEDD (mm)	3.5 ± 0.2	3.6 ± 0.4	3.9 ± 0.2**	4.8 ± 1.0***#	3.9 ± 0.2*	3.6 ± 0.2
LVESD (mm)	2.2 ± 0.3	2.4 ± 0.5	2.7 ± 0.4**	3.8 ± 1.3***#	2.5 ± 0.1*	2.3 ± 0.3
IVSD (mm)	0.69 ± 0.07	0.69 ± 0.10	0.72 ± 0.19	0.80 ± 0.21	0.65 ± 0.06	0.62 ± 0.08
IVSS (mm)	1.1 ± 0.1	1.1 ± 0.1	1.2 ± 0.2	0.8 ± 0.4#	1.1 ± 0.1	1.1 ± 0.2
LVPWD (mm)	0.53 ± 0.11	0.50 ± 0.08	0.64 ± 0.11*	0.50 ± 0.05	0.50 ± 0.08	0.52 ± 0.08
LVPWS (mm)	0.97 ± 0.10	0.87 ± 0.12	0.98 ± 0.25	0.58 ± 0.20*#	0.90 ± 0.14	0.80 ± 0.16
FS (%)	38 ± 3	33 ± 5	32 ± 7*	14 ± 8***##	38 ± 4	36 ± 9
HR (beats/min)	350 ± 54	343 ± 74	312 ± 31	326 ± 72	300 ± 31	303 ± 54

Postpartum (PP), postpartum/BR (PP/BR), and age-matched nulli-pari (NP) females were utilized for these studies. Heart-to-body-weight ratio (HW:BW), LV end-diastolic diameter (LVEDD), end-systolic diameter (LVESD), intraventricular septum thickness in diastole (IVSD) or in systole (IVSS), LV posterior wall thickness in diastole (LVPWD) and systole (LVPWS), fractional shortening (FS), and heart rate (HR) were determined by transthoracic echocardiography in sedated mice. At least five animals per group were investigated for each parameter. Data are represented as mean ± SD, *p < 0.05, **p < 0.01 versus NT-NP, #p < 0.05, and ##p < 0.01 versus NT-PP.

RESULTS

Cardiac-Restricted Deletion of *stat3* Leads to PPCM

Nulli-pari CKO (CKO-NP) and HET females (HET-NP) develop normally and do not show signs of heart failure or increased mortality. At the age of 6 months, cardiac function is normal and comparable with sisters harboring two copies of the floxed *stat3* allele (NT-NP) without the *aMHC-cre^{+/-}* transgene (Table 1, HET-NP, data not shown).

No pregnancy-associated cardiac phenotype or mortality was observed in 20 NT sisters (Figure 1 A) or ten females with only the *cre* transgene (*aMHC-cre^{+/-}*: C+/-PP; Figure 1A and Table S1, in the Supplemental Data available with this article online). Thus, neither the floxed *stat3* allele alone nor *cre* alone had an adverse effect peri- and postpartum. By contrast, physiological stresses of pregnancy, labor, and/or nursing resulted in PPCM in all of the 53 CKO females studied. Roughly two-thirds (37 out of 53 CKO females versus 0 out of 20 NT-PP females, p < 0.01) had died after the second pregnancy (Figure 1A). Notably, no CKO female survived more than five pregnancies. In HET females, PPCM-related death was found after three to four deliveries (Figure 1A). Death occurred always within the first 3 weeks after delivery. After two and four pregnancies, respectively, the majority of CKO and HET females presented signs of overt heart failure, such as generalized edema and labored breathing. The hearts were characterized by four-chamber dilatation, often with thrombi in the atria, extensive fibrosis (Figure 1B), and an increase in cardiomyocyte length (Table S2 and Figure S1). Echocardiography revealed left ventricular (LV) dilatation and depressed fractional shortening in CKO-PP and HET-PP females (Table 1 and Table S3) compared with NT-PP females. CKO-PP females showed increased cardiac mRNA levels of hypoxia inducible factor-1 α (HIF1 α) (Chi and Karliner, 2004) and BNIP3 (Kubasiak et al., 2002) (Figure 1C) and a markedly reduced content of energy-rich phosphates, ATP (-68% ± 7%, p < 0.01 versus NT-PP), and ADP (-57% ± 10%, p < 0.01 versus NT-PP), indicative for cardiac hypoxia. Cardiac apoptosis, as indicated by an increased number of TUNEL-positive cells (cardio-myocytes and nonmyocytes) and protein levels of activated caspase-3 (act-Casp-3), was substantially higher in CKO-PP females compared with NT-PP females (Figures 1D and 1E) or C+/-PP females (Figure S2).

STAT3 Is Activated in the Maternal Heart in Pregnancy and Postpartum

In NT-Prg (day 17 of pregnancy) and NT-PP females, we observed increased Tyr-705 phosphorylation of STAT3 (Figure 1F). As expected, cardiac STAT3 was barely detectable in CKO females (Figure 1F) and STAT3 signals were markedly reduced in the isolated cardiomyocyte-enriched fraction, but not in the nonmyocyte fraction of CKO-PP compared with NT-PP hearts, (Figure S2), indicating that STAT3 activation in LVs from NT-PP mice is mainly occurring in cardiomyocytes. Prolactin (PRL) serum levels increased late in pregnancy and postpartum and are known to activate STAT3 (Cataldo et al., 2000). In fact, infusion of recombinant PRL activated STAT3 in the heart in vivo, and addition of PRL to cultured cardiomyocytes activated STAT3 in vitro (Figure S3).

Figure 1: PPCM in CKO-PP Mice

(A) Survival in relation to number of pregnancies of NT-PP (n = 20), C+/-PP (n = 10), HET-PP (n = 7), and CKO-PP mice (n = 53).

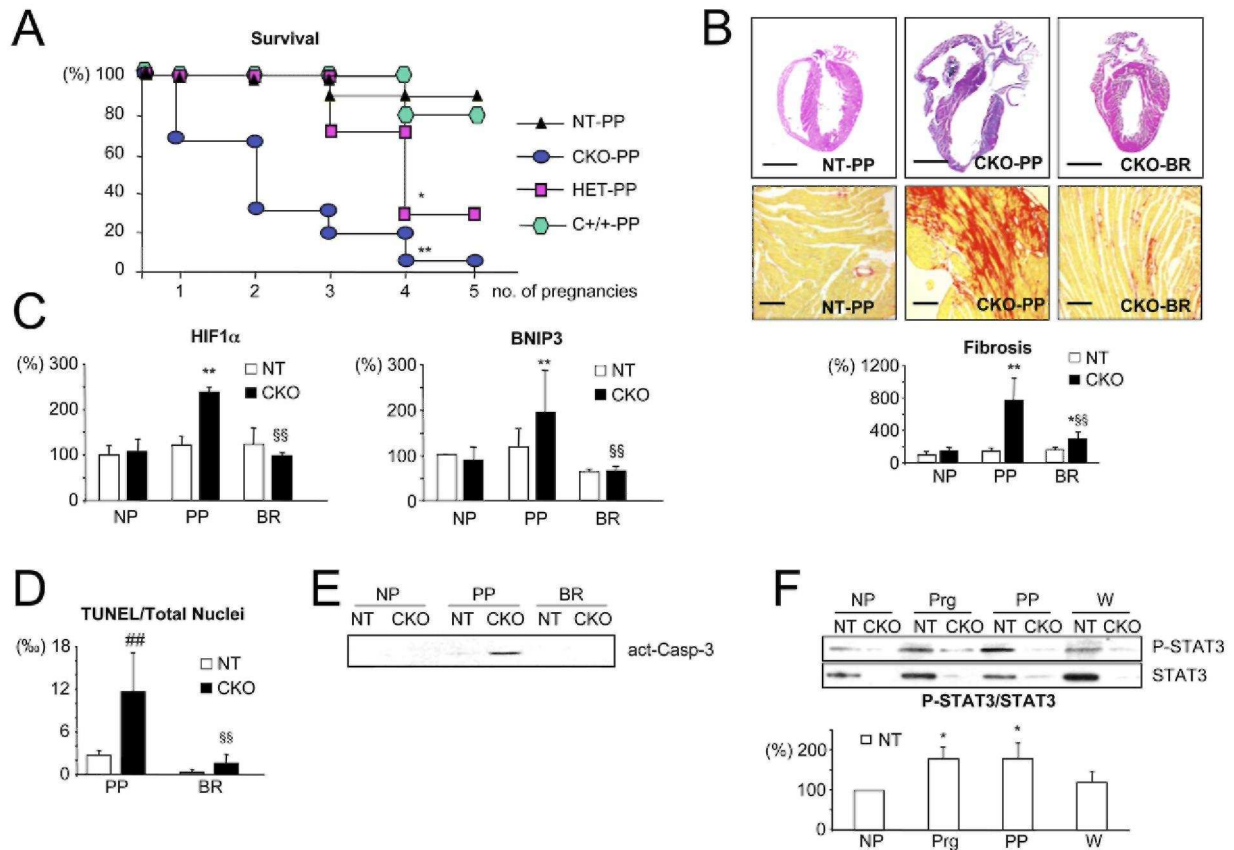
(B) Representative H&E (upper panels) and picro-Sirius red (lower panels) staining in heart sections from a CKO-PP mouse (middle panels), an age- and pregnancy-matched NT-PP mouse (left panels), or a CKO-BR mouse (right panel). Bars in upper panels, 2.5 mm; bars in lower panels, 100 μ m. Bar graph summarizes quantification of fibrosis.

(C and D) Bar graphs summarizing mRNA expression of HIF1 α and BNIP3 (C) or the ratio of TUNEL positive to total number of nuclei in LVs from NT and CKO females (D).

(E) Protein levels of act-Casp-3 in LVs from NT or CKO females.

(F) Protein levels of P-STAT3 and total STAT3 in LVs from NT or CKO mice; the bar graph summarizes the ratio of P-STAT3:STAT3 in LVs from NT females.

In (B)-(H), four to seven mice per group were analyzed. Abbreviations: NP, nulli-pari; Prg, pregnant; PP, postpartum; and W, 4 weeks after weaning. Data are presented as mean \pm SD. * p < 0.05, ** p < 0.01 versus NT-NP, ## p < 0.01 CKO-PP versus NT-PP, and §§ p < 0.01 CKO-BR versus CKO-PP.



Cardiac Deficiency of STAT3 Does Not Affect Pregnancy-Induced Cardiac Hypertrophy

Pregnancy induces a reversible physiological hypertrophy of cardiomyocytes (Eghbali et al., 2005). CKO-Prg and NT-Prg females showed a similar increase in cardiomyocyte growth (cross-sectional area and length; Figure S1 and Table S2), indicative for normal Prg-induced cardiac hypertrophy in CKO-Prg females.

Postpartum Myocardial Angiogenesis Is Impaired in CKO Females

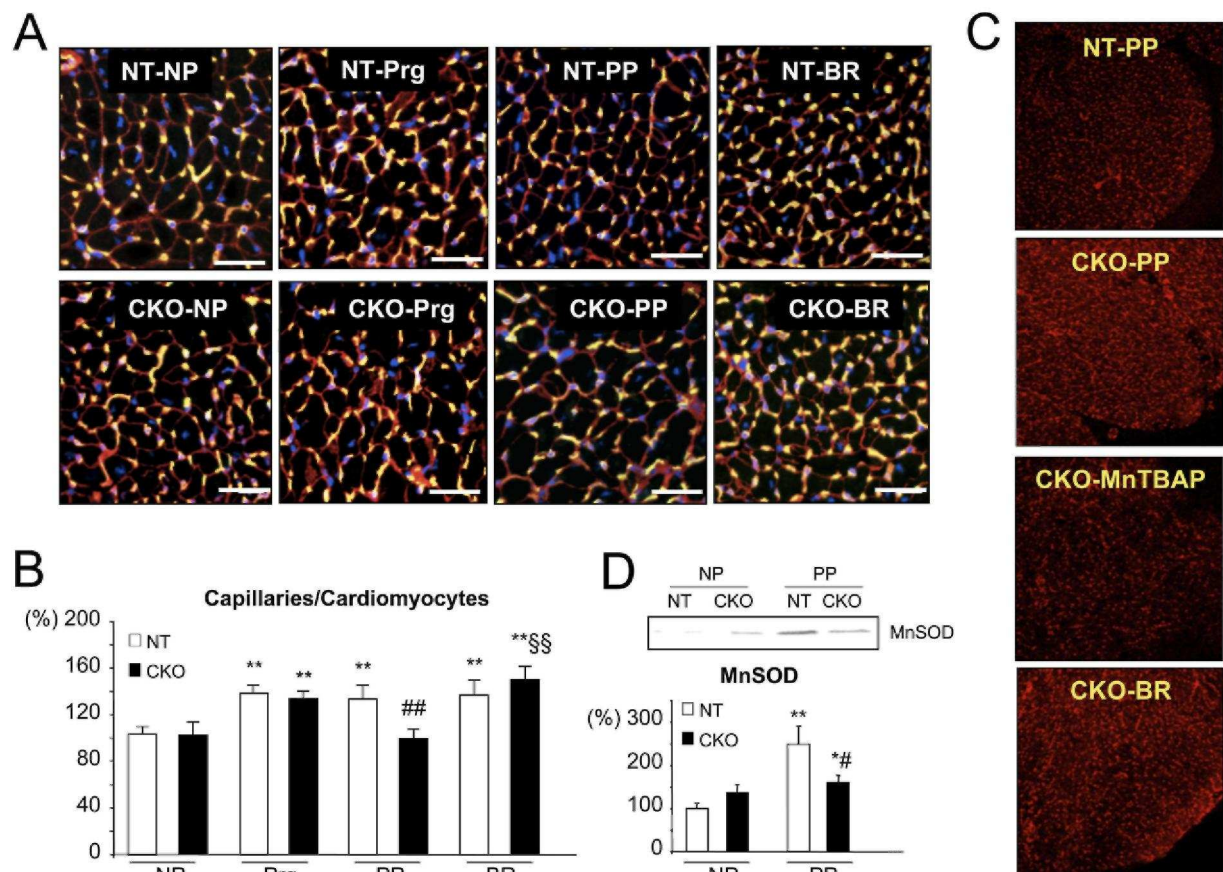
Physiological hypertrophy, as it is observed during pregnancy (Eghbali et al., 2005), requires the proportional growth of the capillary network (Hudlicka and Brown, 1996). In NT-Prg and CKO-Prg females, the ratio of capillaries to cardiomyocytes increased to a similar degree (Figures 2A and 2B). This increased capillary density was maintained in NT-PP females, although it had decreased to prepregnancy levels in CKO-PP females (Figures 2A and 2B). The reduction in the LV capillary density in CKO-PP mice was paralleled with decreased expression of VEGF (CKO-PP: mRNA, $-30\% \pm 15\%$; VEGF protein: $-56\% \pm 22\%$ versus NT-PP, $p < 0.05$) and of von Willebrandt Factor (CKO-PP: vWF mRNA, $-26\% \pm 16\%$ versus NT-PP, $p < 0.05$).

Increased Oxidative Stress in CKO-PP Hearts

STAT3 is known to protect cardiomyocytes from oxidative stress in part by the upregulation of the ROS scavenging enzyme MnSOD (Negoro et al., 2001). NT-PP mice showed a marked increase in cardiac MnSOD protein levels compared to NT-NP, whereas only a moderate increase was observed in CKO-PP females (Figure 2D). Likewise, cardiac MnSOD mRNA levels were higher in NT-PP than CKO-PP females (NT-PP: +54% \pm 1% versus CKO-PP, $p < 0.05$). The production of ROS was enhanced in LVs from CKO-PP compared with NT-PP females as determined by dihydroethidium fluorescence staining, (5 days postpartum: +91% \pm 32% versus NT-PP, $p < 0.05$, Figure 2C; and 3 weeks postpartum CKO-PP: +48% \pm 23% versus NT-PP, $p < 0.05$) and as determined by NADH-stimulated superoxide production measured by electron spin resonance spectroscopy (3 weeks postpartum: CKO-PP: +122% \pm 71% versus NT-PP, $p < 0.05$).

Figure 2: Capillary Density in the Peri- and Postpartum Heart

(A) Capillaries in LV sections of NT-NP, CKO-NP, NT-Prg, CKO-Prg, NT-PP, CKO-PP, NT-BR, and CKO-BR were identified by isolectin B4 immuno-histochemistry (yellow). WGA marks cell membranes (red), and Hoechst stain identifies nuclei (blue) (bars, 40 μ m).
 (B) Bar graph summarizing capillaries per 100 cardiomyocytes in NT and CKO mice; ratios in NT-NP females were set as 100% (CKO-NP, $n = 12$; NT-Prg, $n = 4$; CKO-Prg, $n = 5$; NT-PP, $n = 12$; CKO-PP, $n = 12$; NT-BR $n = 11$; and CKO-BR, $n = 11$). Similar data were obtained with CD31 /WGA staining (data not shown).
 (C) In situ detection of superoxide production with dihydroethidium fluorescence staining (the oxidative dye hydroethidine is red fluorescent when oxidized to EtBr by O_2^-) in LV sections of NT-PP, CKO-PP, CKO-MnTBAP, and CKO-BR females 5 days postpartum.
 (D) Protein levels of MnSOD in NT and CKO mice; the bar graph summarizes MnSOD protein levels ($n = 4-6$ each genotype). Data are presented as mean \pm SD, * $p < 0.05$, ** $p < 0.01$ versus NT-NP, # $p < 0.05$, ## $p < 0.01$ CKO-PP versus NT-PP, and §§ $p < 0.01$ CKO-BR versus CKO-PP.



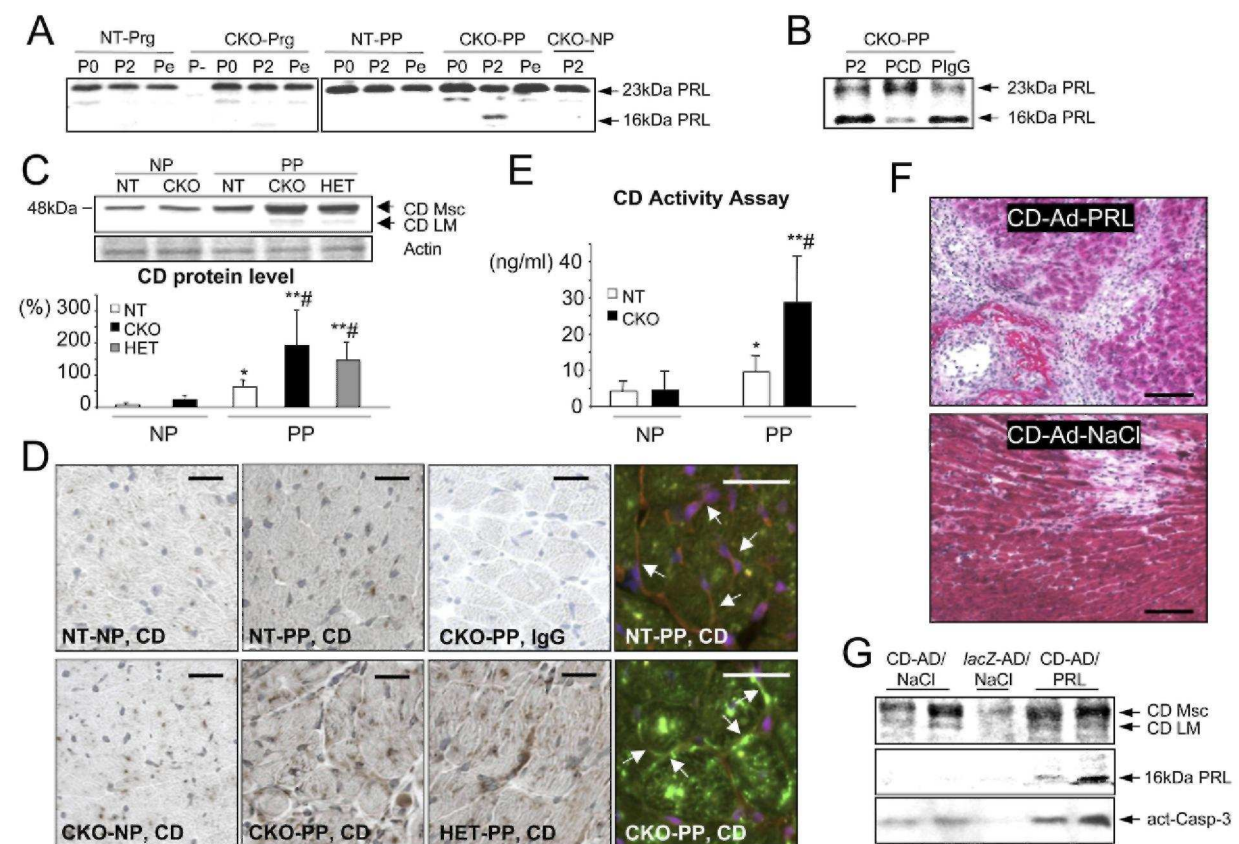
MnTBAP Attenuates PPCM in CKO Mice

We assessed whether the pharmacological suppressor of ROS, tetrakis (4-benzoic acid) porphyrin (MnTBAP), a substance with catalytic activities similar to MnSOD (Houstis et al., 2006), would prevent PPCM. In fact, MnTBAP attenuated ROS generation in CKO females (CKO-MnTBAP: +6% \pm 7% versus NT-PP, n.s.; Figure 2B), the upregulation of activated cathepsin D (CD) and act-Casp-3 protein, and the increase in β -myosin heavy chain (β MHC) mRNA (Figure S4). Moreover, CKO-MnTBAP females showed preserved cardiac capillary density (Figure S4) and cardiac function (Table S4) and displayed no postpartum-related mortality (0% in CKO-

MnTBAP, n = 12, after two subsequent pregnancies). Despite preserved cardiac function, MnTBAP did not prevent the LV dilatation (Table S4) and the upregulation of matrix metalloproteinase 3 (MMP3) mRNA (Figure S4), indicating only a partial suppression of the PPCM phenotype in CKO females.

Figure 3: PRL Cleavage Assay and CD Expression and Activity in LVs of NT and CKO Females

(A) Protein levels of 23 and 16 kDa PRL in NT-Prg, CKO-Prg, NT-PP, CKO-PP, or CKO-NP LV supernatant after incubation with recombinant PRL for 0 hr (P0) or for 2 hr (P2) in the absence or presence of pepstatin A (Pe) or (B) after preabsorption with a neutralizing CD antibody (PCD) or unspecific IgG antibody (PIgG) prior to incubation for 2 hr.
 (C) LV protein levels of CD (CD Msc, mature single-chain; CD LM, large chain of mature double-chain); the bar graph summarizes CD protein levels, and (D) anti-CD staining (brown) and nuclear staining with hematoxylin (blue) in LV sections from NT, CKO and HET females, NP, and PP. IgG served as control for anti-CD specificity. Right panels demonstrate extracellular localization (arrows point to interstitium) of CD in CKO-PP by immunofluorescence staining in a larger magnification (CD, green; WGA, red; and Hoechst, blue); bars, 50 μ m.
 (E) Bar graph summarizing CD activity in NT and CKO LV supernatant.
 (F) H&E-stained LV section from NT-NP mice infected with CD-Ad in the presence (CD-Ad-PRL) or absence (CD-Ad-NaCl) of high levels of recombinant PRL.
 (G) Protein levels of CD, 16 kDa PRL, and act-Casp-3 in LVs from CD-Ad-NaCl, *lacZ*-Ad-NaCl, and CD-Ad-PRL mice. NP, nulli-pari; PP, postpartum. All data are from n = 4-6 individuals per genotype and are presented as mean \pm SD. *p < 0.05, **p < 0.01 versus NT-NP, and #p < 0.05 CKO-PP or HET-PP versus NT-PP. HET-PP mice after four litters.



CD-Dependent Cleavage of PRL in CKO-PP Hearts

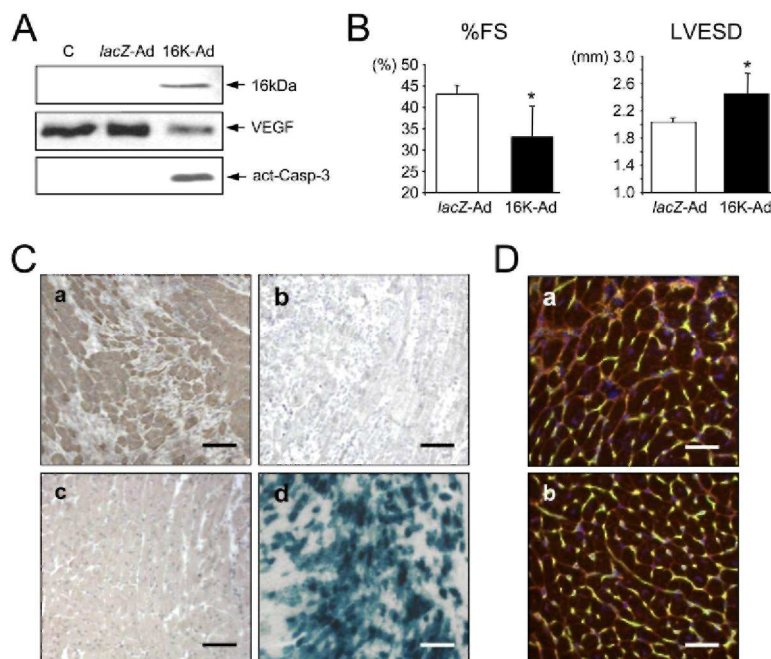
PRL, a dominant hormone in pregnancy and early postpartum, can exert opposing effects on angiogenesis depending on proteolytic processing of the proangiogenic full-length 23 kDa PRL into an antiangiogenic 16 kDa form (Corbacho et al., 2002; Tabruyn et al., 2003). An antibody recognizing both forms of PRL (Lkhider et al., 2004) showed immunoreactivity in LV sections of nursing CKO-PP and NT-PP females, but not in LV sections of NT-NP or CKO-NP females (Figure S5), whereas in western blot analysis, neither this nor other commercially available antibodies against PRL revealed reproducible quantitative or qualitative results. However, in an ex vivo assay (Lkhider et al., 2004) using supernatant of minced LV tissue from CKO-PP females, a high cleavage activity for recombinant PRL into the 16 kDa form was observed, whereas no cleaved 16 kDa PRL was generated from LV tissue extracts of CKO-NP, NT-PP, CKO-Prg, or NT-Prg mice (Figure 3A).

Among the proteolytic enzymes known to process PRL, CD very efficiently cleaves PRL into its 16 kDa form (Corbacho et al., 2002; Tabruyn et al., 2003). In fact, the PRL cleaving activity of CKO-PP LV supernatant was attenuated by preincubation with the CD inhibitor pepstatin A (Lkhider et al., 2004) or by preabsorbing the supernatant with a CD neutralizing antibody (Figures 3A and 3B), implicating that CD is the major PRL cleavage enzyme in CKO-PP hearts.

Oxidative stress promotes the release of CD from lysosomes into the cytosol in cardiomyocytes (Corbacho et al., 2002; Roberg and Ollinger, 1998). Cardiac protein levels of the active single chain mature form of CD (CD Msc) were markedly upregulated in CKO-PP females compared with those in NT-PP, NT-NP, and CKO-NP females (Figure 3C), but expression of activated CD was attenuated in CKO-MnTBAP females (Figure S4). LV sections from NT-NP and CKO-NP females showed weak staining for CD in cardiomyocytes (Figure 3D), whereas marked staining for CD was observed in cardiomyocytes and the LV interstitium of CKO-PP and HET-PP females (Figure 3D). CD cleavage activity was substantially enhanced in super-natants of minced LVs of CKO-PP females compared with CKO-NP or NT-PP females (Figure 3E). Cultured cardiomyocytes infected with a CD expressing adenovirus (CD-Ad) released active CD forms into the cell culture medium, which processed 23 kDa PRL into 16 kDa PRL (Figure S6).

Figure 4: Adenoviral Expression of 16 kDa PRL in Mouse LVs

(A) Protein expression of 16 kDa PRL, VEGF, and act-Casp-3 in LVs from NT females or controls (C) infected with 16K-Ad or *lacZ*-Ad. (B) Bar graphs display reduced percentage of FS and LV dilatation in NT-NP females infected with 16K-Ad (n = 5) compared with females infected with *lacZ*-Ad (n = 5). (C) Anti-PRL staining (brown, [a]) and IgG control (b) in 16K-Ad-infected LV sections. Anti-PRL (c) or *lacZ* (d) staining in *lacZ*-Ad-infected LV tissue sections (bars, 100 μ m). (D) Capillary density identified by staining with isolectin B4 (yellow), WGA (red), and Hoechst (blue) in LV sections from 16K-Ad (a) or *lacZ*-Ad NT-NP females (b) (bars, 50 μ m). Data are presented as mean \pm SD, *p < 0.05.



Prolactin Promotes Cardiac Injury in CD Overexpressing Hearts

We analyzed the effect of locally produced CD in the presence of high systemic PRL levels by injecting a CD expressing adenovirus (CD-Ad) into hearts of NT-PRL or control females (NT-NaCl). Seven days after infection with CD-Ad, NT-PRL mice showed severe cardiac damage (Figure 3F), including elevated levels of act-Casp-3 (Figure 3G) and enhanced mortality compared with NT-NaCl mice infected with CD-Ad (mortality: CD-Ad in NT-PRL, 33%, n = 9; versus 0% in CD-Ad in NT-NaCl, n = 7). Enhanced cardiac CD expression was detected in all CD-Ad-infected mice. PRL, notably mainly the cleaved 16 kDa form, could only be detected in females that were chronically infused with recombinant 23 kDa PRL (Figure 3G).

16 kDa PRL Decreases Myocardial Capillary Density and Reduces Cardiac Function Independent of Pregnancy

To examine the effect of the 16 kDa PRL in the heart, we injected adenoviral vectors expressing human 16 kDa PRL (16K-Ad) or *lacZ* (*lacZ*-Ad) as control into the LV wall of NT-NP females. Two weeks after infection, persistent cardiac expression of 16 kDa PRL was observed in 16K-Ad-infected females that was associated with LV dilatation and decreased cardiac function compared with *lacZ*-Ad-infected females (Figures 4A-4C). The 16 kDa PRL expression was paralleled by decreased cardiac capillary density ($-31\% \pm 12\%$, $p < 0.05$, Figure 4D), reduced VEGF expression, and increased protein levels of act-Casp-3 (Figure 4A). Infection with 16K-Ad did not alter the LV:BW ratio or the cardiomyocyte CSA (Figure S6). In cultured cardiomyocytes, survival was similar after infection with the 16K-Ad or the *lacZ*-Ad (Figure S6). However, 16K-Ad infection of cultured cardiomyocytes impaired their metabolic activity (Figure S6).

Chronic infusion (3 weeks) of recombinant full-length 23 kDa PRL in NT-NP and CKO-NP (NT-PRL and CKO-PRL) in absence of postpartum-associated stress did not affect cardiac function and survival (Table S5). Activation of STAT5 was observed in LVs of NT-PRL and CKO-PRL mice (Figure S3), in line with studies implicating STAT5 as a preferential target for PRL (Cataldo et al., 2000). In addition, stimulation with 23 kDa PRL enhanced the activation of STAT3 in NT-NP hearts in vivo and in cultured cardiomyocytes in vitro (Figure S3). In line with described proangiogenic effects of 23 kDa PRL (Corbacho et al., 2002), the myocardial capillary density was slightly enhanced in NT-PRL and CKO-PRL females (Table S5).

Bromocriptine, an Inhibitor of PRL Secretion, Prevents PPCM in CKO Females

The role of PRL for the development of PPCM was tested by preventing its release from the pituitary glands using bromocriptine (BR), a dopamine-D2-receptor agonist, known to block PRL efficiently in humans (Harrison, 1979) and mice (Nagafuchi et al., 1999). CKO (CKO-BR) and NT (NT-BR) females were treated with BR for two consecutive pregnancies. The efficient blockade of PRL release was confirmed by the following observations: (1) in contrast to NT-PP and CKO-PP females with detectable PRL antigens in LV sections, LV sections from NT-BR and CKO-BR mice were negative for PRL staining (Figure S5), (2) NT-BR and CKO-BR were not able to nurse their offspring because pups appeared underdeveloped three days after birth, and (c) the increased activation of STAT5, the preferential target of PRL, was attenuated in CKO-BR and NT-BR females (Figure S7).

BR prevented postpartum mortality in CKO-BR females (mortality after two pregnancies: 0% in CKO-BR females, $n = 12$ versus 70% in CKO-PP females, $n = 53$, $p < 0.01$) and preserved postpartum angiogenesis (Figures 2A and 2B), cardiac function, and dimensions (Figure 1B, Table 1, and Figure S8). BR also prevented cardiac fibrosis and ap-optosis (Figures 1B, 1D, and 1E), attenuated the mRNA expression of HIF1 α and BNIP3 (Figure 1C) and β MHC and MMP3 (Figure S8), and normalized the expression of α MHC (Figure S8) in CKO-BR females.

BR did not reduce ROS production in the early state (5 days postpartum) of treatment (CKO-BR: $+67\% \pm 9\%$ versus CKO-PP: $91\% \pm 32\%$, n.s., Figure 2C). After 3 weeks of postpartum treatment, however, ROS production in CKO-BR was markedly reduced (CKO-BR: $+7\% \pm 23\%$ versus CKO-PP $48\% \pm 23\%$, $p < 0.05$, Figure S8). In NT-BR females, cardiac function, cardiac angiogenesis, blood pressure, and heart frequency were not affected (Table 1 and Tables S6-S8). Thus, we did not identify direct effects of BR on the myocardium.

Decreased STAT3 Protein Levels in the Myocardium of PPCM Patients

To explore whether STAT3 is involved in human PPCM as well, STAT3 protein levels were quantified in LV tissue obtained from PPCM patients ($n = 5$) at the time of transplantation and compared with levels in similar LV tissues of otherwise normal human hearts ($n = 7$). Figure 5A shows reduced STAT3 protein levels in LVs from patients with PPCM compared with normal human LVs.

Serum of Lactating Women with PPCM Displays Increased oxLDL Levels, Enhanced Activation of CD, and Augmented Protein Levels of the 16 kDa PRL

In the serum of lactating patients with PPCM, levels of oxidized low-density lipoprotein (oxLDL), a marker for oxidative stress (Weinbrenner et al., 2003), and CD activity were enhanced compared with healthy lactating mothers (Figures 5B and 5C). Marked levels of an antigen corresponding to the 16 kDa PRL were detected by western blot (Figure 5D) in the sera of three out of five lactating PPCM patients with obvious cardiac dysfunction at the time of serum sampling (mean percentage of EF, 24 ± 7). It is important to note that the 23 kDa form of PRL was readily detectable, whereas the 16 kDa PRL was barely detectable in healthy lactating women ($n = 5$, Figure 5D).

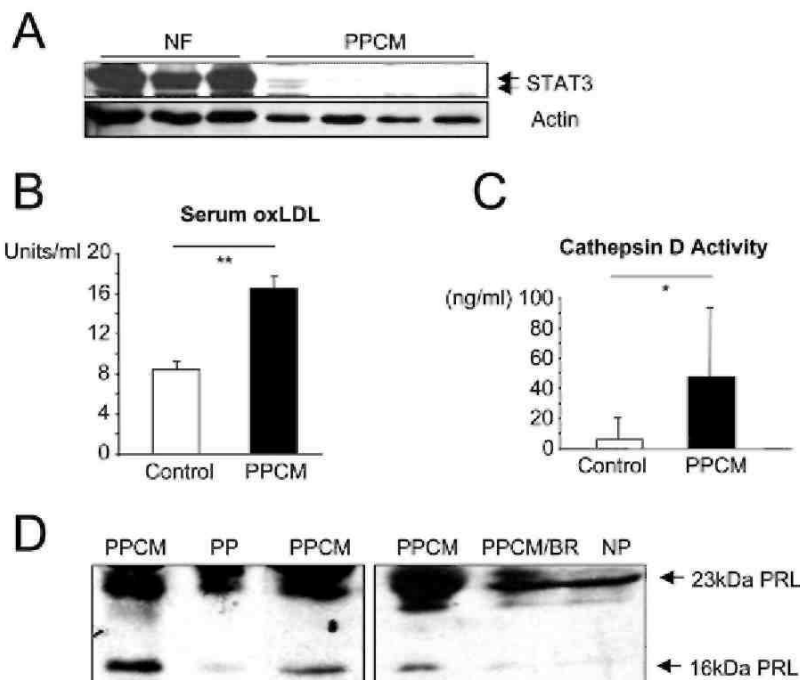
Indication that Bromocriptine Treatment Prevents PPCM in High-Risk Patients

Women with PPCM who recover normal cardiac function have a high risk for recurring PPCM (Sliwa et al., 2004). We therefore initiated a preliminary clinical study in women who had recovered from a previous episode of PPCM and presented with a subsequent pregnancy. Six out of 12 women received BR in addition to standard therapy up to 3 months postdelivery while six patients received standard treatment (peripartum ejection fraction, EF, was similar in both groups; Table S9). In patients receiving BR postdelivery, PRL serum levels, which were elevated more than 5-fold, returned to nonpregnant levels within 14 days of treatment (Figure 5D) as described previously (Harrison, 1979). Three months postpartum, all six

BR-treated women had preserved or increased LV function and dimensions (Table S9) and survived the 4 month observation period. In contrast, the EF in the non-BR-treated (UT) group was deteriorated and three women had died within 4 months (Table S9).

Figure 5: Cardiac STAT3 Expression and Serum Levels of Activated CD and Cleaved 16 kDa PRL in Patients with PPCM

(A) STAT3 protein levels in nonfailing (NF) LVs and in LVs from patients with end-stage heart failure due to PPCM. Total actin served as loading control.
(B) Serum levels of oxLDL in PPCM patients ($n = 29$) and pregnancy matched controls ($n = 21$).
(C) CD activity in nursing PPCM patients ($n = 5$) and in pregnancy matched healthy control women ($n = 5$).
(D) PRL immunoprecipitation followed by detection of 23 kDa and 16 kDa PRL in serum of nursing PPCM patients, healthy nursing women (PP), control women (NP), and women with PPCM after a 14 days treatment with BR (PPCM/BR). Data are presented as mean \pm SD, * $p < 0.05$, and ** $p < 0.01$.



DISCUSSION

We present evidence that pregnancy-related adaptive hypertrophy is associated with enhanced cardiac angiogenesis and that maintenance of the latter in the postpartum phase critically depends on STAT3. The absence of cardiomyocyte STAT3 in the postpartum heart causes increased oxidative stress due to blunted induction of the antioxidant enzyme MnSOD. As a consequence, expression and proteolytic activity of CD are increased, which in turn, induces a detrimental conversion of the nursing hormone PRL into its antiangiogenic 16 kDa derivative. The generation of 16 kDa PRL greatly accelerates the negative effects of oxidative stress and activated CD. In fact, its detrimental effects on the coronary microvasculature promote myocardial hypoxia and apoptosis, thereby contributing to the development of PPCM. Thus, we provide evidence that enhanced activity and release of CD mechanistically connects the increased oxidative stress in STAT3-deficient cardiomyocytes to the development of PPCM. In fact, our study links cardiac processing of PRL into an antiangiogenic and proapoptotic 16 kDa peptide by CD to PPCM and implies that blocking the secretion of PRL can prevent PPCM in mice. Initial clinical observations are consistent with the notion that this beneficial effect of BR may also apply to patients with PPCM.

Enhanced myocardial capillary density is part of the physiological hypertrophy, which the maternal heart undergoes to compensate for the increased volume and workload during pregnancy and labor. Because NT-Prg and CKO-Prg female mice showed increased myocardial capillary density late in pregnancy, this process seems to be independent from cardiomyocyte STAT3. Increased myocardial capillary density is maintained up to 3 weeks postpartum in NT-PP females. In CKO-PP females, however, enhanced myocardial capillary density is lost in the postpartum phase, implying a novel role of STAT3 as a key requisite for maintaining postpartum myocardial an-giogenesis. Failure of this process leads to hypoxia as indicated by the increased expression of the hypoxia marker genes HIF1 α (Chi and Karliner, 2004) and BNIP3 (Kubasiak et al., 2002), a lower content of energy rich phosphates, apoptosis, and subsequently, heart failure.

Increased hemodynamic load, occurring during pregnancy and labor, may promote cardiac hypoxia and oxidative stress in CKO mice. However, we never observed symptoms or death in CKO females during pregnancy or at delivery, when hemodynamic load culminates. Likewise, increased hemodynamic load induced by aortic constriction did not affect cardiac hypertrophy, function, and mortality in CKO-NP females (Table S10). Cardiomyocyte hypertrophic growth during pregnancy was maintained, suggesting that cardiomyocyte hypertrophy induced by hemodynamic load is not affected in CKO females and therefore does not appear to be the primary trigger for PPCM in CKO mice.

STAT3 and Akt signaling are known to promote hypertrophy and angiogenesis and to exert protection from apoptosis in the heart (Hilfiker-Kleiner et al., 2004a; Jacoby et al., 2003; Liao, 2004; Negoro et al., 2001) and may therefore have overlapping protective functions in the myocardium. Indeed, we observed a late increase in Akt activation in pregnancy in both genotypes, which was followed by a postpartum deactivation (Supplemental Data). In contrast to Akt, cardiac activation of STAT3 was enhanced in NT females late in pregnancy and postpartum, at least in part as consequence of increased peri- and postpartum serum levels of full-length PRL, because we demonstrated that PRL stimulation activated STAT3 in the heart *in vivo* and in cardiomyocytes *in vitro*. Taken together, during pregnancy, elevated Akt activation may ensure physiological adaptation of the heart toward pregnancy-related stress, and this might be sufficient to protect CKO-Prg females despite the lack of STAT3. In NT-PP females, activated STAT3 seems to be sufficient to maintain postpartum cardioprotection; in contrast, the lack of both Akt and STAT3 activation in CKO-PP is detrimental, indicating that among several putative mechanisms (including Akt), STAT3 signaling is necessary for protecting the heart from development of PPCM.

Oxidative stress is known to rise during pregnancy, culminating in the last trimester, and is paralleled by an increase in total antioxidant capacity (Toescu et al., 2002). The antioxidant capacity in normal pregnancies peaks in the postpartum phase, suggesting a need for an efficient antioxidant defense mechanism postpartum (Toescu et al., 2002). Circulating levels of oxLDL are markers of oxidative stress in patients (Weinbrenner et al., 2003). In contrast to normal postpartum women, serum levels of oxLDL in patients with PPCM were elevated, indicating enhanced oxidative stress in these patients. Moreover, LVs from CKO-PP mice display an enhanced production of superoxide anions, suggesting that the lack of cardiomyocyte STAT3 impairs important defense mechanisms against postpartum-related oxidative stress. Indeed, it has been shown that MnSOD, a powerful ROS scavenging enzyme, is under the transcriptional control of STAT3 in cardiomyocytes (Negoro et al., 2001). MnSOD plays a crucial role in the antioxidant defense of the heart, because only a 50% decrease in MnSOD protein levels in heterozygous *mnsod*^{+/-} mice is associated with increased oxidative damage and cardiomyocyte death (Van Remmen et al., 2001). Notably, although this reduction of MnSOD protein levels is associated with subtle alterations in cardiomyocyte mitochondrial functions alone, it is not sufficient to induce cardiomyopathy under basal conditions (Van Remmen et al., 2001). Pregnancy/postpartum-associated stress, however, leads to

cardiomyopathy in heterozygous *mnsod*^{+/-} females (Figure S10). Thus, a 50% reduction of MnSOD protein appears to be sufficient to cause peri/postpartum cardiomyopathy. In fact, we observed that LVs from NT-PP mice showed higher levels of MnSOD mRNA and proteins than LVs from CKO-PP mice, indicating a STAT3-dependent transcriptional regulation of MnSOD in the postpartum heart. In line with a lower oxidative defense, CKO-PP LVs displayed enhanced superoxide anion production, which could be prevented with a pharmacological enhancement of MnSOD-like enzyme activity by treatment of CKO mice with MnTBAP. In addition, MnTBAP prevented cardiac dysfunction and postpartum mortality in CKO mice. Thus, STAT3, via inducing MnSOD expression, promotes important defense mechanisms against oxidative stress in the postpartum heart.

The PPCM phenotype of our mouse model showed a degeneration of the cardiac capillary network, which was prevented by treatment with MnTBAP or by blocking the release of PRL by BR. It has been shown that oxidative stress enhances the expression and activation of CD (Cor-bacho et al., 2002; Roberg and Ollinger, 1998), an enzyme known to cleave full-length 23 kDa PRL into its antiangiogenic 16 kDa form (Lkhider et al., 2004). The 16 kDa PRL is able to dissociate endothelial cell structures, to impair endothelium-dependent vasorelaxation, and to promote apoptosis in endothelial cells and is considered as a physiological inhibitor of tumor growth (Corbacho et al., 2002; Gonzalez et al., 2004; Tabruyn et al., 2003). Large quantities of pituitary PRL are released into the circulation during lactation (Lkhider et al., 2004), and it has been shown that cleavage of PRL into the 16 kDa form by CD takes place in the extracellular compartment of the mammary glands under physiological conditions (Lkhider et al., 2004). Cardiac levels of active CD protein were markedly increased and detected in the interstitium of CKO-PP mice. The observation that active CD released from CD overexpressing hearts in vivo or from cultured cardiomyocytes released in vitro processes 23 kDa PRL into its 16 kDa form together with the finding that PRL cleavage activity could be blocked by a neutralizing CD antibody in CKO-PP LV supernatant ex vivo strongly suggest that CD is mainly responsible for the generation of 16 kDa PRL. In addition, lowering oxidative stress by MnTBAP prevented the up-regulation of activated CD in postpartum CKO females. Therefore, we postulate that oxidative stress enhances CD activity and leads to proteolytic cleavage of PRL in the myocardium of CKO-PP females.

Adenoviral expression of the 16 kDa PRL in the heart reduced cardiac capillary density and cardiac function independently of pregnancy and nursing and, indeed, recapitulates aspects of the cardiac phenotype of PPCM. In contrast to its destructive effect on endothelial cells (Corbacho et al., 2002; Gonzalez et al., 2004; Tabruyn et al., 2003), the 16 kDa PRL did not affect cardiomyocyte survival. However, it attenuated cardiomyocyte metabolic activity and may therefore directly affect cardiomyocyte function, an aspect that will be evaluated in future studies.

Myocardial injury by CD overexpression after adenoviral transfection was markedly enhanced in the presence of high systemic PRL levels due to the generation of 16 kDa PRL. Moreover, the systemic toxicity of oxidative stress induced by doxorubicin treatment was enhanced in the presence of high systemic PRL levels (Supplemental Data). Thus, the generation of 16 kDa PRL greatly accelerates cardiac injury caused by oxidative stress and CD. Accordingly, the blockade of PRL release by BR prevented the capillary degeneration and the PPCM phenotype in CKO-BR females. Taken together, we propose that the generation of the antiangiogenic 16 kDa PRL by CD-mediated cleavage of the 23 kDa PRL plays a detrimental role for the cardiac microvasculature and, conceivably, for cardiomyocyte metabolism (Figure 6).

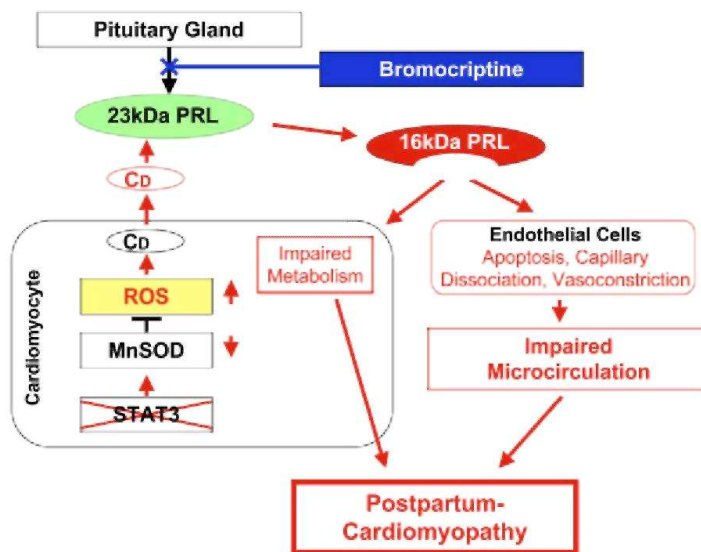
In contrast to the MnTBAP treatment, which prevented cardiac capillary degeneration, but not ventricular dilatation, BR provided a more complete rescue of CKO mice from PPCM, including the prevention of ventricular dilatation and the associated upregulation of MMP3. MMP3 has been implicated in ventricular dilatation (Tziakas et al., 2005) and is responsible for a wide range of extracellular matrix degradation and activation of other MMPs (Mu-kherjee et al., 2005). PRL via activation of STAT5 is able to induce MMP3 expression, a process that can be abolished by BR (Nagafuchi et al., 1999). In fact, attenuated MMP3 expression in CKO-BR mice was associated with a reduction in STAT5 activation, suggesting that a PRL-mediated imbalance of STAT transcription factors in the CKO hearts may, independently from oxidative stress, contribute to the development of PPCM. Further studies will be required to test this hypothesis.

Although STAT3 is markedly reduced in the myocardium from patients with PPCM, our data do not provide information as to whether this reduction of STAT3 is a primary or a secondary event of PPCM. Nevertheless, similar to our observation in CKO mice, reduced STAT3 may contribute to the development and/or progression of PPCM in patients. So far, sequence analysis of the *stat3* gene in the DNA samples from patients with PPCM and controls did not reveal polymorphisms in the STAT3 gene associated with PPCM (Monika Stoll, personal communication). Our findings of increased CD activity, elevated levels of oxLDL, and 16 kDa PRL in serum

samples of nursing PPCM patients, but not in pregnancy-matched controls, point to striking similarities between our PPCM mouse model and human PPCM and are consistent with the notion that oxidative stress, CD activation, and subsequent PRL cleavage may also contribute to the development of PPCM in patients. Our encouraging initial results in a preliminary clinical study with patients treated with BR, a drug widely used to stop lactation in postpartum women (Harrison, 1979), are consistent with the hypothesis that PRL and mainly the 16 kDa PRL are causally related to the development of PPCM in patients. As a limitation of this study, it should be noted that not all effects of BR on its targets were analyzed and that the inhibition of PRL secretion is the most plausible reason for the protective effect of BR in PPCM.

Figure 6: Schematic Model for the Development of PPCM

In the absence of cardiomyocyte STAT3 activity, the postpartum expression of MnSOD is attenuated, leading to increased oxidative stress and the release of CD, which processes 23 kDa PRL into its detrimental 16 kDa form. 16 kDa PRL induces endothelial cell apoptosis, capillary dissociation, and vasoconstriction and impairs cardiomyocyte metabolism, thereby promoting PPCM. Accordingly, BR, a pharmacologic inhibitor of PRL release, prevents PPCM in mice by decreasing circulating PRL.



In summary, we show that STAT3 plays a critical role for the preservation of postpartum myocardial angiogenesis and function and suggest a central role of STAT3 and associated signaling pathways in the onset of PPCM (Figure 6). Importantly, we present evidence for a novel mechanism for the development of cardiomyopathy, which involves the cleavage of PRL into its detrimental 16 kDa form by CD (Figure 6). BR, a pharmacological inhibitor of PRL release, prevents PPCM in mice (Figure 6). In consequence, based on our experimental and initial clinical findings, BR may represent a novel therapeutic option to treat patients with PPCM or to prevent the disease in patients who suffered and recovered from PPCM in a previous pregnancy.

EXPERIMENTAL PROCEDURES

PRL (sheep), BR, and all other chemicals were purchased from Sigma.

Cardiomyocyte-Specific Deletion of *stat3*

The generation of mice with cardiomyocyte-restricted deletion of *stat3* has been described (Hilfiker-Kleiner et al., 2004a). Female mice were first bred at the age of 10-12 weeks, at an age when STAT3 protein was barely detectable in isolated cardiomyocytes (Figure S2), indicating that, as in CKO males (Hilfiker-Kleiner et al., 2004a), the Cre-mediated deletion of *stat3* was virtually complete.

Animal Experiments

Generally, analyses were performed 3 weeks after the second delivery. Prolactin (400 iU/kg) was injected i.v. For chronic administration, osmotic minipumps (Alzet; PRL 400 iU/kg/d) were implanted in sedated mice. Adenoviruses, 16K-Ad (Pan et al., 2004), *JacZ*-Ad, or CD-Ad (3×10^8 pfu of each virus) was injected directly into the mouse LV (Supplemental Experimental Procedures). BR (4 mg/kg/d, Novartis) was added in drinking water. MnTBAB (300 μ g/mouse/day) or vehicle (placebo) was injected subcutaneously. Transthoracic

echocardiography was performed in sedated mice as previously described (Hilfiker-Kleiner et al., 2004a). Hemodynamic measurements were assessed by telemetry (Pelat et al., 2003) or tail cuff in conscious mice or by Millar catheter in anesthetized mice as described previously (Hilfiker-Kleiner et al., 2004a, 2004b). For more detailed description of animal experiments, see the Supplemental Experimental Procedures.

All animal studies were in compliance with the *Guide for the Care and Use of Laboratory Animals* as published by the U.S. National Institutes of Health and were approved by our local Institutional Review Boards.

Patients Data

LV samples were from patients undergoing heart transplantation due to PPCM (NYHA functional class III or IV) and from donor hearts (NF) that could not be transplanted for technical reasons. Serum was obtained from PPCM patients (NYHA functional class III or IV) at their first presentation and from age and pregnancy-matched nursing healthy woman. oxLDL was determined with a sandwich ELISA kit (Mercodia). More detailed patient data are presented in the Supplemental Experimental Procedures.

Histological Analyses and Immunostaining

For histological analyses, hearts were fixed in situ, embedded in paraffin, and stained with picro-Sirius red or H&E, as described (Hilfiker-Kleiner et al., 2004a). Interstitial collagen volume fraction was determined in picro-Sirius red-stained sections as described (Hilfiker-Kleiner et al., 2004a). Apoptotic nuclei were detected by in situ terminal deoxynucleotidyl transferase-mediated digoxigenin-conjugated dUTP nick end labeling (TUNEL) and by nuclear morphology using Hoechst 33258 staining (Hilfiker-Kleiner et al., 2004a).

Capillary Density

Capillary density was determined as the ratio of capillaries to 100 cardiomyocytes in transversely sectioned LV tissue immunostained with isolectin B4 (Vector) or the platelet-endothelial cell adhesion molecule-1 (PECAM-1) antibody (Santa Cruz) and counterstained with WGA and Hoechst 33258 as described previously (Hilfiker-Kleiner et al., 2004a).

Measurement of Myocardial Superoxide Production and NADH activity

Dihydroethidium fluorescence staining was used for in situ detection of superoxide production as described (Engberding et al., 2004). NADH activity was determined in LV myocardium (50 µg protein) by electron spin resonance (ESR) spectroscopy as described previously (Spiekermann et al., 2003). Both methods are described in the Supplemental Experimental Procedures.

Measurement of Energy-Rich Phosphates in Myocardial Tissue

AMP, ADP, and ATP were measured as described previously (Hilfiker-Kleiner et al., 2004a). A brief description is provided in the Supplemental Experimental Procedures.

CD Activity Assay

Supernatant from freshly isolated LV tissue was generated by mincing LV tissue in ice-cold HBSS. Sedimented minced LV tissue was then incubated in DMEM for 1 hr at 37°C and 5% CO₂. CD activity was determined in LV supernatant or in patient serum by using the InnoZyme CD Immunocapture Activity Assay Kit (Calbiochem) and a FLUOstar Galaxy.

PRL Cleavage Assay

PRL cleavage activity was assayed in LV supernatant (described above) by adding citrate/phosphate buffer (pH 3.5) at a 1:1 ratio; subsequently, pepstatin A (2 mg/L) and/or recombinant PRL (0.1 g/L) was added and mixed and incubated at 37°C (5% CO₂) for 2 hr. After addition of an equal volume of Laemmli buffer (5% BME, 0.2% DTT), samples were assayed by immunoblotting. For depletion of CD protein, LV supernatant was incubated with a CD neutralizing antibody (Nr. 06-467, Upstate) and subsequently protein A-agarose (Roche) to sediment and remove CD from supernatant.

Real-Time PCR and Immunoblot Analyses

Real-time measurements of PCR amplification were performed by using the Stratagene MX4000 multiplex QPCR System using the SYBR green dye method (Brilliant SYBR Green Mastermix-Kit, Stratagene) as described (Klein et al., 2005). Primer sequences are listed in the Supplemental Experimental Procedures. Protein expression levels were determined by western blotting according to standard procedures; antibodies are listed in the Supplemental Experimental Procedures.

Statistical Analyses

Data are presented as mean \pm SD. Differences between groups were analyzed by Mann-Whitney test, log-rank test, Student's t test, or ANOVA followed by Bonferroni as appropriate. A two-tailed p value of <0.05 was considered to indicate statistical significance.

Supplemental Data

Supplemental Data include Supplemental Experimental Procedures, Supplemental References, ten figures, and ten tables and can be found with this article online at <http://www.cell.com/cgi/content/full/128/3/589/DC1/>.

ACKNOWLEDGMENTS

We are indebted to Silvia Gutzke, Birgit Brandt, Ewa Kolka, and Philipp Fischer for expert technical assistance. We thank Prof. Dr. Joseph Martial from the Université de Liege, Belgium for fruitful discussions. *mnsod*^{+/-} and WT females were kindly provided by Dr. Ting-Ting Huang, Palo Alto VA Medical Center, CA. This study was supported by the Jean Leducq Foundation, the Deutsche Forschungsgemeinschaft, Deutscher Akademischer Austausch Dienst, and the Foundation for Polish Science.

REFERENCES

- Bartoli, M., Platt, D., Lemtalsi, T., Gu, X., Brooks, S.E., Marrero, M.B., and Caldwell, R.B. (2003). VEGF differentially activates STAT3 in microvascular endothelial cells. *FASEB J.* *17*, 1562-1564.
- Cataldo, L., Chen, N.Y., Yuan, Q., Li, W., Ramamoorthy, P., Wagner, T.E., Sticca, R.P., and Chen, W.Y. (2000). Inhibition of oncogene STAT3 phosphorylation by a prolactin antagonist, hPRL-G129R, in T-47D human breast cancer cells. *Int. J. Oncol.* *17*, 1179-1185.
- Chi, N.C., and Karliner, J.S. (2004). Molecular determinants of responses to myocardial ischemia/reperfusion injury: focus on hypoxia-inducible and heat shock factors. *Cardiovasc. Res.* *61*, 437-447.
- Corbacho, A.M., Martinez De La Escalera, G., and Clapp, C. (2002). Roles of prolactin and related members of the prolactin/growth hormone/placental lactogen family in angiogenesis. *J. Endocrinol.* *173*, 219-238.
- Eghbali, M., Deva, R., Alioua, A., Minosyan, T.Y., Ruan, H., Wang, Y., Toro, L., and Stefani, E. (2005). Molecular and functional signature of heart hypertrophy during pregnancy. *Circ. Res.* *96*, 1208-1216.
- Elkayam, U., Akhter, M.W., Singh, H., Khan, S., Bitar, F., Hameed, A., and Shotan, A. (2005). Pregnancy-associated cardiomyopathy: clinical characteristics and a comparison between early and late presentation. *Circulation* *111*, 2050-2055.
- Engberding, N., Spiekermann, S., Schaefer, A., Heineke, A., Wiencke, A., Muller, M., Fuchs, M., Hilfiker-Kleiner, D., Hornig, B., Drexler, H., and Landmesser, U. (2004). Allopurinol attenuates left ventricular remodeling and dysfunction after experimental myocardial infarction: a new action for an old drug? *Circulation* *110*, 2175-2179.
- Gonzalez, C., Corbacho, A.M., Eiserich, J.P., Garcia, C., Lopez-Barrera, F., Morales-Tlalpan, V., Barajas-Espinosa, A., Diaz-Munoz, M., Rubio, R., Lin, S.H., et al. (2004). 16K-prolactin inhibits activation of endothelial nitric oxide synthase, intracellular calcium mobilization, and endothelium-dependent vasorelaxation. *Endocrinology* *145*, 5714-5722.
- Harrison, R.G. (1979). Suppression of lactation. *Semin. Perinatol.* *3*, 287-297.
- Hayakawa, Y., Chandra, M., Miao, W., Shirani, J., Brown, J.H., Dorn, G.W., 2nd, Armstrong, R.C., and Kitsis, R.N. (2003). Inhibition of cardiac myocyte apoptosis improves cardiac function and abolishes mortality in the peripartum cardiomyopathy of $\alpha(q)$ transgenic mice. *Circulation* *108*, 3036-3041.
- Hilfiker-Kleiner, D., Hilfiker, A., Fuchs, M., Kaminski, K., Schaefer, A., Schieffer, B., Hillmer, A., Schmiedl, A., Ding, Z., Podewski, E., et al. (2004a). Signal transducer and activator of transcription 3 is required for myocardial capillary growth, control of interstitial matrix

deposition, and heart protection from ischemic injury. *Circ. Res.* 95, 187-195.

Hilfiker-Kleiner, D., Kaminski, K., Kaminska, A., Fuchs, M., Klein, G., Podewski, E., Grote, K., Kiian, I., Wollert, K.C., Hilfiker, A., and Drexler, H. (2004b). Regulation of proangiogenic factor CCN1 in cardiac muscle: impact of ischemia, pressure overload, and neurohumoral activation. *Circulation* 109, 2227-2233.

Houstis, N., Rosen, E.D., and Lander, E.S. (2006). Reactive oxygen species have a causal role in multiple forms of insulin resistance. *Nature* 440, 944-948.

Hudlicka, O., and Brown, M.D. (1996). Postnatal growth of the heart and its blood vessels. *J. Vasc. Res.* 33, 266-287.

Jacoby, J.J., Kalinowski, A., Liu, M.G., Zhang, S.S., Gao, Q., Chai, G.X., Ji, L., Iwamoto, Y., Li, E., Schneider, M., et al. (2003). Cardiomyocyte-restricted knockout of STAT3 results in higher sensitivity to inflammation, cardiac fibrosis, and heart failure with advanced age. *Proc. Natl. Acad. Sci. USA* 100, 12929-12934.

Klein, G., Schaefer, A., Hilfiker-Kleiner, D., Oppermann, D., Shukla, P., Quint, A., Podewski, E., Hilfiker, A., Schroder, F., Leitges, M., and Drexler, H. (2005). Increased collagen deposition and diastolic dysfunction but preserved myocardial hypertrophy after pressure overload in mice lacking PKCepsilon. *Circ. Res.* 96, 748-755.

Kubasiak, L.A., Hernandez, C.M., Bishopric, N.H., and Webster, K.A. (2002). Hypoxia and acidosis activate cardiac myocyte death through the Bcl-2 family protein BNIP3. *Proc. Natl. Acad. Sci. USA* 99, 12825-12830.

Kunisada, K., Negoro, S., Tone, E., Funamoto, M., Osugi, T., Yamada, S., Okabe, M., Kishimoto, T., and Yamauchi-Takahara, K. (2000). Signal transducer and activator of transcription 3 in the heart transduces not only a hypertrophic signal but a protective signal against doxorubicin-induced cardiomyopathy. *Proc. Natl. Acad. Sci. USA* 97, 315-319.

Liao, J.K. (2004). Statin therapy for cardiac hypertrophy and heart failure. *J. Investig. Med.* 52, 248-253.

Lkhider, M., Castino, R., Bouguyon, E., Isidoro, C., and Ollivier-Bousquet, M. (2004). Cathepsin D released by lactating rat mammary epithelial cells is involved in prolactin cleavage under physiological conditions. *J. Cell Sci.* 117, 5155-5164.

Mukherjee, R., Bruce, J.A., McClister, D.M., Jr., Allen, C.M., Sweter-litsch, S.E., and Saul, J.P. (2005). Time-dependent changes in myocardial structure following discrete injury in mice deficient of matrix metalloproteinase-3. *J. Mol. Cell. Cardiol.* 39, 259-268.

Nagafuchi, H., Suzuki, N., Kaneko, A., Asai, T., and Sakane, T. (1999). Prolactin locally produced by synovium infiltrating T lymphocytes induces excessive synovial cell functions in patients with rheumatoid arthritis. *J. Rheumatol.* 26, 1890-1900.

Negoro, S., Kunisada, K., Fujio, Y., Funamoto, M., Darville, M.I., Eizirik, D.L., Osugi, T., Izumi, M., Oshima, Y., Nakaoka, Y., et al. (2001). Activation of signal transducer and activator of transcription 3 protects cardiomyocytes from hypoxia/reoxygenation-induced oxidative stress through the upregulation of manganese superoxide dismutase. *Circulation* 104, 979-981.

Osugi, T., Oshima, Y., Fujio, Y., Funamoto, M., Yamashita, A., Negoro, S., Kunisada, K., Izumi, M., Nakaoka, Y., Hirota, H., et al. (2002). Cardiac-specific activation of signal transducer and activator of transcription 3 promotes vascular formation in the heart. *J. Biol. Chem.* 277, 6676-6681.

Pan, H., Nguyen, N.Q., Yoshida, H., Bentzien, F., Shaw, L.C., Rentier-Delrue, F., Martial, J.A., Weiner, R., Struman, I., and Grant, M.B. (2004). Molecular targeting of antiangiogenic factor 16K hPRL inhibits oxygen-induced retinopathy in mice. *Invest. Ophthalmol. Vis. Sci.* 45, 2413-2419.

Pelat, M., Dessy, O., Massion, P., Desager, J.P., Feron, O., and Balligand, J.L. (2003). Rosuvastatin decreases caveolin-1 and improves nitric oxide-dependent heart rate and blood pressure variability in apolipoprotein E^{-/-} mice in vivo. *Circulation* 107, 2480-2486.

Reimold, S.C., and Rutherford, J.D. (2001). Peripartum cardiomyopathy. *N. Engl. J. Med.* 344, 1629-1630.

Roberg, K., and Ollinger, K. (1998). Oxidative stress causes relocation of the lysosomal enzyme cathepsin D with ensuing apoptosis in neonatal rat cardiomyocytes. *Am. J. Pathol.* 152, 1151-1156.

Sliwa, K., Skudicky, D., Candy, G., Bergemann, A., Hopley, M., and Sareli, P. (2002). The addition of pentoxifylline to conventional therapy improves outcome in patients with peripartum cardiomyopathy. *Eur. J. Heart Fail.* 4, 305-309.

Sliwa, K., Forster, O., Zhanje, F., Candy, G., Kachope, J., and Essop, R. (2004). Outcome of subsequent pregnancy in patients with documented peripartum cardiomyopathy. *Am. J. Cardiol.* 93, 1441-1443.

Sliwa, K., Fett, J., and Elkayam, U. (2006). Peripartum cardiomyopathy. *Lancet* 368, 687-693.

Spiekermann, S., Landmesser, U., Dikalov, S., Brecht, M., Gamez, G., Tatge, H., Reepschlager, N., Hornig, B., Drexler, H., and Harrison, D.G. (2003). Electron spin resonance characterization of vascular xanthine and NAD(P)H oxidase activity in patients with coronary artery

disease: relation to endothelium-dependent vasodilation. *Circulation* 107, 1383-1389.

Tabruyn, S.P., Sorlet, C.M., Rentier-Delrue, F., Bours, V., Weiner, R.I., Martial, J.A., and Struman, I. (2003). The antiangiogenic factor 16K human prolactin induces caspase-dependent apoptosis by a mechanism that requires activation of nuclear factor-kappaB. *Mol. Endocrinol.* 17, 1815-1823.

Toescu, V., Nuttall, S.L., Martin, U., Kendall, M.J., and Dunne, F. (2002). Oxidative stress and normal pregnancy. *Clin. Endocrinol. (Oxf.)* 57, 609-613.

Tziakas, D.N., Chalikias, G.K., Papaioakeim, M., Hatzinikolaou, E.I., Stakos, D.A., Tentes, I.K., Papanas, N., Kortsaris, A., Maltezos, E., and Hatseras, D.I. (2005). Comparison of levels of matrix metalloproteinase-2 and -3 in patients with ischemic cardiomyopathy versus nonischemic cardiomyopathy. *Am. J. Cardiol.* 96, 1449-1451.

Van Remmen, H., Williams, M.D., Guo, Z., Estlack, L., Yang, H., Carlson, E.J., Epstein, C.J., Huang, T.T., and Richardson, A. (2001). Knockout mice heterozygous for Sod2 show alterations in cardiac mitochondrial function and apoptosis. *Am. J. Physiol. Heart Circ. Physiol.* 281, H1422-H1432.

Weinbrenner, T., Cladellas, M., Isabel Covas, M., Fito, M., Tomas, M., Senti, M., Bruguera, J., and Marrugat, J. (2003). High oxidative stress in patients with stable coronary heart disease. *Atherosclerosis* 168, 99-106.